Experimental and theoretical approaches to understanding two-photon absorption spectra in polymethine and squaraine molecules

Jie Fu, Lazaro A. Padilha, David J. Hagan, and Eric W. Van Stryland

College of Optics and Photonics: CREOL & FPCE, University of Central Florida, Orlando, Florida 32816, USA and Department of Physics, University of Central Florida, Orlando, Florida 32816, USA

Olga V. Przhonska and Mikhail V. Bondar

Institute of Physics, National Academy of Sciences, Prospect Nauki 46, Kiev 03028, Ukraine

Yuriy L. Slominsky and Alexei D. Kachkovski

Institute of Organic Chemistry, National Academy of Sciences, Murmanskaya 5, Kiev 03094, Ukraine

Received July 20, 2006; accepted August 21, 2006;
posted September 25, 2006 (Doc. ID 73222); published December 20, 2006

We performed a detailed experimental investigation and quantum-chemical analysis of two-photon absorption (2PA) spectra of a series of symmetrical cationic polymethines and neutral squaraines having similar structures. Degenerate 2PA spectra of these molecules are taken by using two-photon fluorescence spectroscopy and the *Z*-scan technique. All measurements are made with 150 fs laser pulses of 1 kHz repetition rate in the tuning range of 520–2100 nm (0.6–2.4 eV). Comparing 2PA spectra of polymethines and squaraines, we find that we can access considerably larger 2PA cross sections ($\geqslant 8600 \times 10^{-50}$ cm^4 s/photon) in the squaraines owing to narrower linear absorption spectra and an increase in the density of unoccupied molecular orbitals introduced by the squaraine acceptor group in the conjugated chain.

OCIS codes: 190.4180, 190.4710.

1. INTRODUCTION

The development of new organic materials for two-photon absorption (2PA) is an area of ongoing research owing to a number of promising practical applications.[1] Even though there has been considerable progress in the studies of structure-property relationships of organic molecules, much more remains to be discovered. Recent studies from various research groups have shown design strategies for efficient 2PA by a systematic investigation of the conjugation length of the chromophores, various symmetrical and asymmetrical combinations of electron-donor and electron-acceptor terminal groups, and the addition of such groups in the middle of the chromophore to vary the charge distribution.[2–6] Advanced quantum-chemical techniques have been applied to analyze the 2PA response in a series of π-conjugated molecules with different backbones: stilbene, distirylbenzene, polyene, and indenofluorene.[7,8] It has been shown that donor (D)–acceptor (A)–donor (D) quadrupolar-type arrangements of organic molecules are highly desirable to increase 2PA cross sections (δ_{2PA}).[7,8] Polymethine dyes (PDs) and squaraine dyes (SDs) are attractive candidates for 2PA studies owing to their very large ground-state transition dipole moments, near-parallel orientation of their ground- and excited-state transition dipole moments,[9] and the sharply rising low-energy side of their linear absorption spectra that allow significant intermediate state resonance enhancement of the 2PA.[10]

In this work we perform experimental and quantum-chemical studies of four representative organic molecules: two cationic polymethines and two neutral squaraines with analogous structures to provide a deeper insight into the nature of the 2PA processes. We discuss the difference in 2PA spectra for these molecules and uncover the origin of the high $\delta_{2PA} \geqslant 8600 \times 10^{-50}$ cm^4 s/photon (8600 GM) observed for squaraine molecules.

In the following sections we describe: (1) the structure and one-photon (1PA) absorption properties of polymethines and squaraines, (2) the experimental methods used for 2PA and one-photon anisotropy measurements, (3) a detailed analysis of the 2PA spectra, and (4) their quantum-chemical modeling allowing us to understand the nature of the 2PA bands. We find that we can experimentally access larger 2PA cross sections in squaraine dyes than in polymethines owings to an extra 2PA band and a narrower linear absorption spectra produced by adding the squaraine acceptor group in the conjugated chain.

0740-3224/06/010067-10/$15.00

2. EXPERIMENTAL

A. Materials

The molecular structures and linear absorption spectra of the dyes studied in this work, recorded with a Varian Cary 500 spectrophotometer, are shown in Figs. 1–4. Their chemical names are: 2-[5-(1,3-dihydro-3,3-dimethyl-1-propyl-2H-indol-2-ylidene)-1,3-pentadienyl]-3,3-dimethyl-1-propyl-3H-indolium iodide (labeled as PD 2350); 2-[5-(3-ethyl-1,3-dihydro-1,1-dimethyl-2H-benzo[e]indol-2-ylidene)-1,3-pentadienyl]-3-ethyl-1,1-dimethyl-1H-benzo[e]indolium p-toluen sulfonate (labeled as PD 2630); 2-[(3,3-dimethyl-1-propyl-1,3-dihydro-2H-indol-2-ylidene) methyl]-4-[(3,3-dimethyl-1-propyl-3H-indolium-2-yl) methylene]-3-oxocyclobut-1-en-1-olate (labeled as SD 2577), and 2-[(3-butyl-1,1-dimethyl-1,3-dihydro-2H-benzo[e]indol-2-ylidene) methyl]-4-[(3-butyl-1,1-dimethyl-1H-benzo[e]indol-2-yl) methylene]-3-oxocyclobut-1-en-1-olate (labeled as SD 2243). The main spectroscopic properties of the cationic PDs studies in this work are determined by the existence of a delocalized π-electron system in the polymethine chromophore (or polymethine chain) and symmetric terminal groups with equal electron-donor strengths. PDs 2350 and 2630 can be considered as D–π conjugation (A)–D systems. The main distinguishing feature of the neutral squaraines is the C_4O_2 acceptor group inserted into the center of the polymethine chain. The indolium (or benzoindolium) terminal groups are identical, and the length of the π-conjugation is similar for polymethine and squaraine molecules. These dyes were synthesized at the Institute of Organic Chemistry, Kiev, Ukraine, by standard methods as described in Ref. 11. Their molecular structures were confirmed by elemental analysis and nuclear magnetic resonance spectra. As can be seen in Figs. 1–4, the main absorption bands, $S_0 \rightarrow S_1$, are positioned approximately in the same spectral range. The extinction coefficients

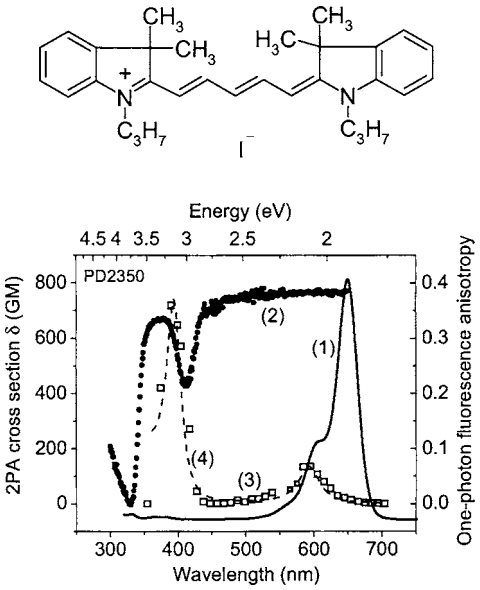

Fig. 1. Molecular structure: (1) linear absorption spectrum, (2) one-photon excitation anisotropy, (3) 2PA spectrum for PD 2350 in ethanol, (4) theoretical curve based on a one-intermediate-state and two-final-states model. Uncertainties in 2PA measurements: ±20%.

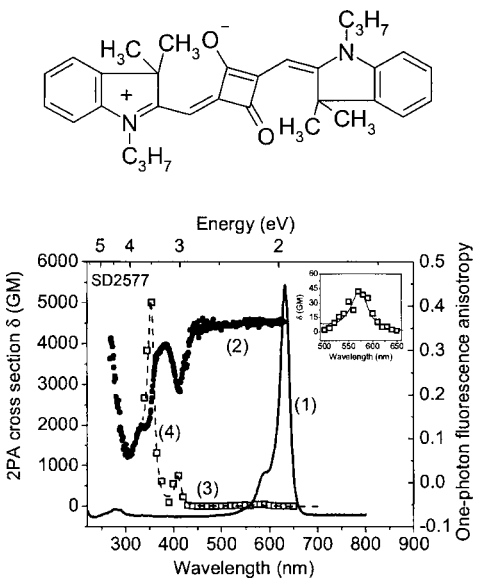

Fig. 2. Molecular structure: (1) linear absorption spectrum in ethanol, (2) one-photon excitation anisotropy in glycerol, (3) 2PA spectrum in ethanol for SD 2577, (4) theoretical curve based on a one-intermediate-state and three-final-states model. Uncertainties in 2PA measurements: ±20%.

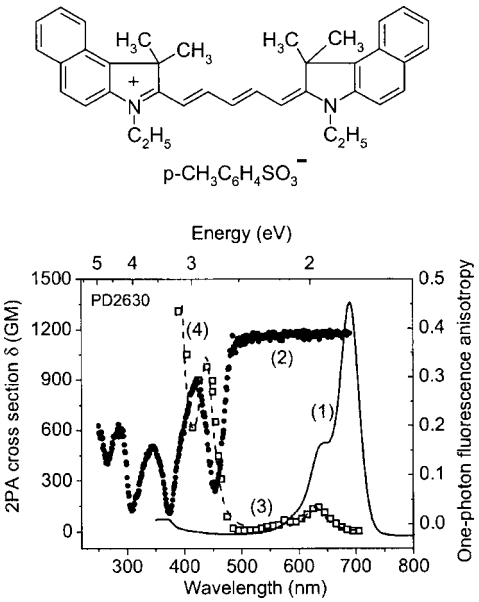

Fig. 3. Molecular structure: (1) linear absorption spectrum in ethanol, (2) one-photon excitation anisotropy in glycerol, (3) 2PA spectrum in ethanol for PD 2630, (4) theoretical curve based on a one-intermediate-state and two-final-states model. Uncertainties in 2PA measurements: ±20%.

are: $2.36\times10^5\ M^{-1}\,cm^{-1}$ at the peak position of 650 nm for PD 2350 in ethanol, $2.12\times10^5\ M^{-1}\,cm^{-1}$ at peak position 688 nm for PD 2630 in ethanol, $3.08\times10^5\ M^{-1}\,cm^{-1}$ at peak position 632 nm for SD 2577 in ethanol, and $3.45\times10^5\ M^{-1}\,cm^{-1}$ at peak position 668 nm for SD 2243 in dichloromethane. SD 2243 does not dissolve well in ethanol, therefore most of the linear and nonlinear measurements for this dye were done in dichloromethane.

B. Experimental Methods

It is commonly known that one-photon anisotropy measurements, especially linked to quantum-chemical calcu-

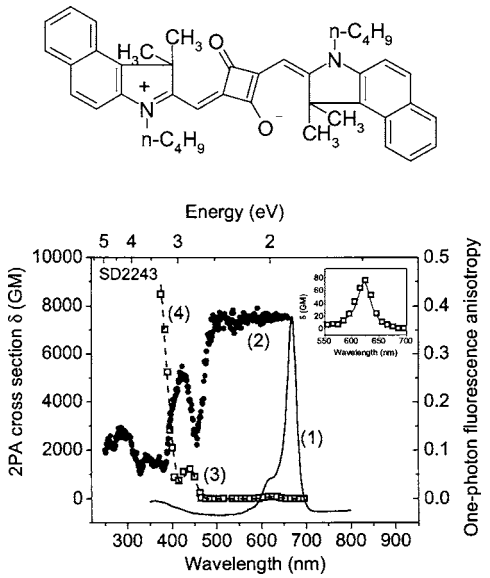

Fig. 4. Molecular structure: (1) linear absorption spectrum in dichloromethane (2) one-photon excitation anisotropy in glycerol, (3) 2PA spectrum in dichloromethane for SD 2243, (4) theoretical curve based on a one-intermediate-state and three-final-states model. Uncertainties in 2PA measurements: ±20%.

lations, can reveal the spectral positions and orientations of the transition dipole moments from the ground state, S_0, to the first excited state, S_1 (μ_{01}), and to the higher excited states S_n (μ_{0n}) relative to the orientation of the emission dipole moment (μ_{10}). This information cannot be obtained from 1PA spectra. For polymethines and squaraines, one-photon anisotropy values, r_{1PA} within the first absorption band are typically close to the theoretical maximum of 0.4, indicating that μ_{01} is almost parallel to μ_{10}. In this case, one-photon anisotropy measurements determine the mutual orientation of different absorbing dipoles, which is important for understanding 2PA processes. Steady-state one-photon fluorescence anisotropy spectra of organic dyes were measured in high-viscosity glycerol solutions to avoid reorientation and in low concentration solutions ($C \approx 10^{-6}$ M) to avoid reabsorption with a Photonic Technology International Quantamaster Spectrofluorimeter. The excitation anisotropy spectrum, $r(\lambda)$, can be calculated as a function of the excitation wavelength λ at a fixed emission wavelength, usually near a fluorescence maximum, as $r(\lambda)=[I_{\parallel}(\lambda)-I_{\perp}(\lambda)]/[I_{\parallel}(\lambda)+2I_{\perp}(\lambda)]$, where $I_{\parallel}$ and $I_{\perp}$ are the fluorescence intensities polarized parallel and perpendicular to the excitation light polarization.[12] The angle between the absorption and emission dipole moments (β) can be determined from one-photon anisotropy values using the following expression: $r_{1PA}=(3\cos^2\beta-1)/5$. In the range $0° \leqslant \beta \leqslant 90°$, one-photon anisotropy values range is $-0.2 \leqslant r_{1PA} \leqslant 0.4$. Fluorescence quantum yields of PDs and SDs in solutions were measured by using a standard method[13] relative to Rhodamine 6G (quantum yield is 0.96 in ethanol[14]).

Frequency degenerate 2PA spectra of the sample solutions were measured by two methods: single-wavelength open-aperture Z-scan[15] and upconverted fluorescence.[13] In both experiments we used linear polarized excitation from a Clark-MXR, CPA2010, Ti:sapphire regenerative amplified system followed by an optical parametric amplifier (model TOPAS 4/800, Light Conversion) providing laser pulses of ~140 fs (FWHM) duration with a 1 kHz repetition rate. The tuning range of the system used in these experiments is 520–2100 nm (0.6–2.4 eV). The Z-scan allows the determination of 2PA cross sections from a simple fitting procedure.[16] This method was applied for the measurements within the stronger second and third 2PA bands. The faster and more sensitive method of upconverted fluorescence was applied to measure a weak 2PA band within the first linear absorption band, which is a symmetry-forbidden transition for 2PA in centrosymmetric SDs that have C_{2i} symmetry, and is only slightly allowed for symmetrical PDs (C_{2v}). Upconverted fluorescence from the molecules was measured in a 10 mm thick quartz cuvette with the same PTI Quantamaster Spectrofluorimeter. 2PA cross sections were measured and calibrated against well-known reference standards: Fluorescein in water (pH=11) and Rhodamine B in methanol.[13]

For each wavelength we check that the fluorescence signal is quadratically dependent on incident irradiance, which is indicative of a pure 2PA process. Any linear component of this dependence is indicative of some linear absorption-induced fluorescence. For wavelengths where this linear absorption affects the upconverted fluorescence we cannot use this method, and we use Z-scan instead. Linear absorption may easily be accounted for in the Z-scan experiment; however, linear absorption can produce excited-state absorption (ESA), which gives a Z-scan signal that is similar to that from 2PA.[17] To ensure that ESA is not affecting our results, we must perform time-resolved pump–probe experiments.[18] ESA typically has a relaxation time much longer than our 150 fs laser pulses, while 2PA is instantaneous.

Experimental results for one-photon anisotropy and 2PA spectra are shown in Figs. 1–4 and discussed in Section 3.

C. Methodology of Quantum-Chemical Calculations

Quantum-chemical calculations were performed with the goal of understanding the spectral position of 2PA bands and revealing the origin of the high 2PA cross section δ_{2PA} in squaraine molecules. For the calculations of the positions of the electronic levels and the shapes of the molecular orbitals (MOs), a well-known molecular orbital as a linear combination of atomic orbitals (MOLCAO) method was used.[19] The wave function of the ith MO φ_i was written as an expansion of the atomic orbitals χ_μ: $\varphi_i = \Sigma_\mu C_{i\mu}\chi_\mu$, where the $C_{i\mu}$ are the corresponding coefficients, and the summation runs over all atomic orbitals. We note that $C_{i\mu}^2$ is the probability of the location of an electron in the ith MO in the neighborhood of the μth atom.[19] Calculations were performed in the framework of the standard semi-empirical approximations (HyperChem package). The equilibrium molecular geometries were calculated employing the Austin Model 1 (AM1) method with the gradient 0.01 kcal/mol. It was established previously that the lengths of the carbon–carbon bonds calculated in this method are in good agreement with the corresponding values obtained by an *ab initio* approximation.[20] The π-system of all molecules was found

to be planar. Characteristics of the electron transitions were obtained in the ZINDO/S approximation with spectral parameterization. The wave function of the pth excited state, Ψ_p, was built as an expansion of the electron configurations, $\Phi_{i\to j}$, corresponding to electron transfer from the occupied ith to vacant jth orbital: $\psi_p = \Sigma_{i,j} T_{p,i\to j} \Phi_{i\to j}$, where $T_{p,i\to j}$ are the normalized coefficients, and indices i and j run over all MOs.[17] $\Sigma_{i,j} T^2_{p,i\to j} = 1$ is a normalization condition. In our calculations we used all $\pi\to\pi^*$ single-excited configurations with the overlap weight factor equal to 0.5. All calculations were performed on isolated molecules neglecting solvent effects.

3. EXPERIMENTAL RESULTS AND DISCUSSION

Experimental one- and two-photon absorption as well as one-photon excitation fluorescence anisotropy spectra are presented in Fig. 1 for PD 2350, in Fig. 2 for SD 2577, in Fig. 3 for PD 2630, and in Fig. 4 for SD 2243. Our measurements show the existence of a weakly allowed 2PA band within the vibronic shoulder of the first absorption band $S_0\to S_1$, for which the transition is forbidden by dipole selection rules for these symmetrical molecules. It is commonly accepted that two-photon excitation to S_1 involves two dipole moments: μ_{01} and $\Delta\mu$ (vector difference between the permanent S_0 and S_1 dipoles). According to the traditional quantum-chemical theories,[19] for all symmetrical polymethine dyes (symmetry C_{2v}) $\Delta\mu$ is oriented perpendicular to μ_{01} or equal to zero for the symmetrical squarylium dyes (symmetry C_{2i}) prohibiting 2PA to the S_1 state. However, this weakly allowed 2PA band was already observed for symmetrical cyanines and cyanine-like molecules (squaraines, Rhodamine B, fluorescein) and explained by the effect of vibronic coupling partly breaking the molecular symmetry and thus the dipole selection rules.[13,14,21] This symmetry-breaking effect was also confirmed by our measurements of two-photon anisotropy in PDs (See Ref. 22 for details). Cross sections for these weak 2PA bands are: 140 GM for PD 2350 (peak position at ≈590 nm), 40 GM for SD 2577 (peak position at ≈570 nm), 160 GM for PD 2630 (peak position at ≈625 nm), and 85 GM for SD 2243 (peak position at ≈625 nm). We note that cross sections for squaraine dyes are smaller than for polymethines, which may be connected with their different molecular symmetry. As was already mentioned, symmetrical polymethine dyes have C_{2v} symmetry and a nonzero $\Delta\mu$ value. As a result, this band is slightly allowed by dipole selection rules in contrast to being a forbidden band in the centrosymmetrical SDs with $\Delta\mu = 0$.

Considering the more intense 2PA bands, our measurements for PD 2350 revealed the position of the second 2PA band at ≈390 nm with $\delta_{2PA} \approx 720$ GM. Note the sharp decrease in 2PA values at 355 nm. Analysis of one-photon excitation fluorescence anisotropy, $r(\lambda)$, for PD 2350 revealed the alternation of the allowed and forbidden (by symmetry) one-photon transitions. One-photon forbidden transitions, as transitions between states of the same symmetry, can indicate a possible position of 2PA bands. A first dip in $r(\lambda)$ was observed at 412 nm ($r_{1PA} = 0.22$) corresponding to the angle $\beta \approx 33°$ between μ_{01} and μ_{10}. However, the peak of 2PA for PD 2350 is shifted to the blue region by ≈22 nm relative to this anisotropy dip. A second dip in $r(\lambda)$ at 330 nm ($r_{1PA} \approx 0$) corresponds to the angle $\beta \approx 55°$. Since this wavelength is almost exactly half that of the absorption peak in the $S_0\to S_1$ transition, i.e., double-resonance, degenerate 2PA into this band would be enhanced by an intermediate state resonance.[9] However, as we observe from Fig. 1, this double resonance cannot be reached by 2PA owing to the influence of linear absorption.

Figure 2 shows the analogous information for SD 2577. In contrast to PD 2350, the experimentally observed 2PA spectrum for SD 2577 includes 3 bands: a weakly allowed band at the vibronic shoulder of the $S_0\to S_1$ transition, a more intense band at ≈408 nm with $\delta_{2PA} \approx 760$ GM, and a much more intense band at ≈350 nm with $\delta_{2PA} \approx 5200$ GM. The 2PA spectrum for this molecule can be directly mapped onto the anisotropy function $r(\lambda)$. The observed dips at 410 nm ($r_{1PA} = 0.22$, $\beta \approx 33°$) and at 345 nm ($r_{1PA} = 0.13$, $\beta \approx 42°$) correspond to the peak positions of the 2PA bands. Analogous to PD 2350, the last dip at 309 nm ($r_{1PA} = 0.06$, $\beta \approx 49°$), corresponding to a position of twice the energy of the main allowed $S_0\to S_1$ absorption band (or double-resonance position). The 2PA cross section at this dip (the corresponding excitation wavelength is 618 nm) cannot be experimentally determined due to 1PA, the same reason we discussed for PD 2350.

The 2PA spectrum for PD 2630, presented in Fig. 3, is more complicated than that for PD 2350. In contrast to PD 2350, there is no strong decrease in δ_{2PA} after the second 2PA band ($\delta_{2PA} \approx 920$ GM at 440 nm). We observe an increase in δ_{2PA} to ≈1320 GM at 390 nm (corresponding to the shortest excitation wavelength of 780 nm), and this increase in δ_{2PA} may be the beginning of a third 2PA band. This new band is connected with the larger π conjugation length in the benzoindolium terminal groups, and will be discussed more in Section 4. Similar to PD 2350, there is a shift of ≈13 nm between the second 2PA peak (440 nm) and the first one-photon excitation fluorescence anisotropy dip at 453 nm.

Figure 4 shows the 2PA spectrum for SD 2243 with the same terminal groups as for PD 2630. The 2PA trends for both dyes are similar. For the second 2PA peak at 440 nm, SD 2243 shows a similar value of $\delta_{2PA} \approx 1200$ GM, however, for the next 2PA band, δ_{2PA} is considerably larger, reaching ≈8660 GM at 375 nm, which is experimentally observed with the shortest possible excitation wavelength of 750 nm allowed by linear absorption. The peak position and strength of this 2PA band cannot be resolved for the same reason as for PD 2630, i.e., linear absorption loss.

4. QUANTUM-CHEMICAL APPROACH

Quantum-chemical calculations have been performed with the goal of understanding the 2PA spectra for cationic polymethines and neutral squaraines having analogous structures and for uncovering the origin of the high δ_{2PA} experimentally observed for squaraine molecules. For these purposes we consider the evolution of the electronic levels and transitions from the unsubstituted polymethine chain: $H_2C^+-(CH=CH)_2-CH=CH_2$ to the cat-

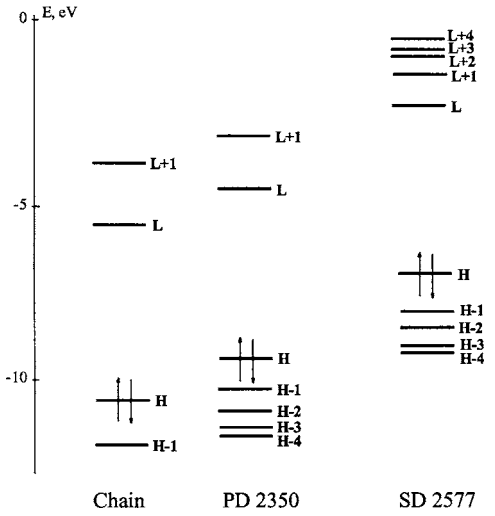

Fig. 5. Scheme of the electronic levels for the unsubstituted chain PD 2350 and SD 2577.

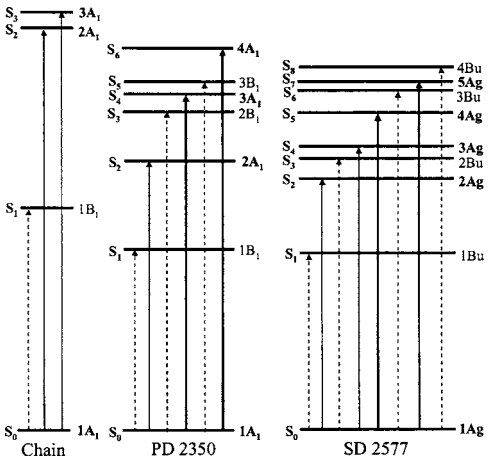

Fig. 6. Scheme of the electronic transitions for the unsubstituted chain PD 2350 and SD 2577. Dashed lines, one-photon allowed transitions; solid lines, allowed two-photon transitions; bold solid lines, experimentally observed two-photon transitions.

ionic PD 2350 and neutral SD 2577. Schemes of some higher-occupied and lower-unoccupied MOs, as well as the corresponding transitions between them, are presented in Figs. 5 and 6. The shapes of highest occupied molecular orbital (HOMO)−1, HOMO, lowest unoccupied molecular orbital (LUMO) and LUMO+1 for the polymethine chain are presented in Fig. 7(a). The calculated characteristics are collected in Table 1. In our considerations we limit the number of MOs to the number of electronic transitions participating in one- and two-photon absorption between $S_0 \rightarrow S_1$ and its double resonance position.

A. Polymethines

Quantum-chemical calculations of the unsubstituted polymethine chain show in Fig. 6 that the ground-state to the first excited-state transition, $S_0 \rightarrow S_1$, is allowed by symmetry rules ($1A_1 \rightarrow 1B_1$) and is connected with the electron transfer between the HOMO and LUMO. The two next electronic transitions, $S_0 \rightarrow S_2$ ($1A_1 \rightarrow 2A_1$) and $S_0 \rightarrow S_3$ ($1A_1 \rightarrow 3A_1$), are forbidden and correspond to the combination of HOMO−1→LUMO and HOMO→LUMO+1 with quite different oscillator strengths (see Table 1). These transition energies are close but not exactly equal to each other. The calculated spectral shift between the corresponding $S_0 \rightarrow S_2$ and $S_0 \rightarrow S_3$ absorption bands is $\approx$20 nm, i.e., no degeneracy. This is the origin of the main difference between the spectra of the cationic polymethine chain and its neutral polyene analogue. The polyene chain is characterized by the formation of double (for $A_u \rightarrow A_u$) and triple (for $B_g \rightarrow B_g$) degenerate configurations leading to splitting and to a redistribution of oscillator strengths.[7] This makes the least-energetic transition disallowed for 1PA but allowed for 2PA. For the polymethine chain, one of the $A_1 \rightarrow A_1$ transitions approximately corresponds to a double-resonance position of the main absorption band, which makes it impossible to reach the 2PA peak experimentally, again owing to linear absorption. We emphasize that all MOs in the unsubstituted conjugated polymethine chain are totally and uniformly delocalized, and all electronic transitions are described mainly by single configurations with coefficients $T_{p,i \rightarrow j} > 0.9$ (see Table 1).

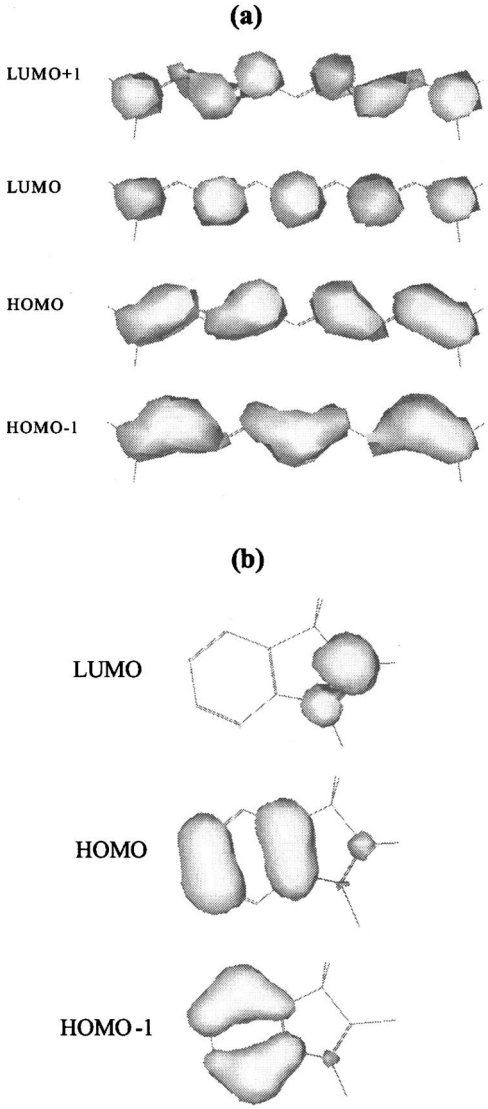

Fig. 7. Electron density distribution in the MOs of the (a) unsubstituted chain and the (b) terminal groups.

Table 1. Calculated Parameters for the Unsubstituted Polymethine Chain PD 2350 and SD 2577

Dye	Transition	λ, nm	Oscillator Strength	Symmetry of Final State	Main Configuration
Unsubstituted Chain	$S_0 \rightarrow S_1$	551	1.65	B_1	$0.96\|\mathrm{H}\rightarrow\mathrm{L}\rangle$
	$S_0 \rightarrow S_2$	315	0.002	A_1	$0.97\|\mathrm{H\text{-}1}\rightarrow\mathrm{L}\rangle$
	$S_0 \rightarrow S_3$	291	0.08	A_1	$0.97\|\mathrm{H}\rightarrow\mathrm{L+1}\rangle$
PD 2350	$S_0 \rightarrow S_1$	655	1.6	B_1	$0.96\|\mathrm{H}\rightarrow\mathrm{L}\rangle$
	$S_0 \rightarrow S_2$	460	0.01	A_1	$0.94\|\mathrm{H\text{-}1}\rightarrow\mathrm{L}\rangle$
	$S_0 \rightarrow S_3$	410	0.07	B_1	$0.92\|\mathrm{H\text{-}2}\rightarrow\mathrm{L}\rangle$
	$S_0 \rightarrow S_4$	395	0.02	A_1 (local)	$0.95\|\mathrm{H\text{-}3}\rightarrow\mathrm{L}\rangle$
	$S_0 \rightarrow S_5$	386	0.06	B_1	$0.93\|\mathrm{H\text{-}4}\rightarrow\mathrm{L}\rangle$
	$S_0 \rightarrow S_6$	352	0.05	A_1	$0.95\|\mathrm{H}\rightarrow\mathrm{L+1}\rangle$
SD 2577	$S_0 \rightarrow S_1$	630	1.7	B_u	$0.97\|\mathrm{H}\rightarrow\mathrm{L}\rangle$
	$S_0 \rightarrow S_2$	480	0	A_g	$0.87\|\mathrm{H\text{-}1}\rightarrow\mathrm{L}\rangle$
	$S_0 \rightarrow S_3$	465	0.005	B_u	$0.85\|\mathrm{H\text{-}2}\rightarrow\mathrm{L}\rangle$
	$S_0 \rightarrow S_4$	456	0.34	A_g (O–O)	$0.45\|\mathrm{H}\rightarrow\mathrm{L+2}\rangle+0.85\|\mathrm{H}\rightarrow\mathrm{L+3}\rangle$
	$S_0 \rightarrow S_5$	410	0	A_g	$0.87\|\mathrm{H}\rightarrow\mathrm{L+1}\rangle$
	$S_0 \rightarrow S_6$	386	0.03	B_u	$0.54\|\mathrm{H\text{-}4}\rightarrow\mathrm{L}\rangle+0.66\|\mathrm{H}\rightarrow\mathrm{L+3}\rangle$
	$S_0 \rightarrow S_7$	384	0	A_g (local)	$0.96\|\mathrm{H\text{-}3}\rightarrow\mathrm{L}\rangle$
	$S_0 \rightarrow S_8$	378	0.2	B_u	$0.63\|\mathrm{H\text{-}4}\rightarrow\mathrm{L}\rangle+0.52\|\mathrm{H}\rightarrow\mathrm{L+3}\rangle$

Introduction of the donor indolium terminal groups (TGs) to the polymethine chain to form the PD 2350 increases the density of the occupied MOs and thus the number of electronic transitions, which is a subject of interest. Figure 7(b) presents three MOs (HOMO−1, HOMO, and LUMO) belonging to each TG. Interaction of the MOs of all molecular fragments (chain and two TGs) in PD 2350 leads to the delocalization of the three highest occupied MOs (HOMO, HOMO−1, and HOMO−2 shown in Fig. 8), not only along the polymethine chain but also extended through the TGs. Therefore, the introduction of the indolium TGs with their own conjugated systems causes a considerable and effective lengthening of the chromophore. Calculations show that below these totally delocalized MOs, there is a HOMO−3 that is located primarily on the benzene rings of the TGs and thus can be considered as a local MO. This orbital is placed comparatively close to the LUMO, and the electronic transition HOMO−3→LUMO (corresponding to $S_0 \rightarrow S_4$, $1A_1 \rightarrow 3A_1$ in Fig. 6 for PD2350) appears in the interval between the states S_1 and S_6. The existence of the local MO is of great importance for 2PA. Note that LUMO and LUMO+1 extend the chain conjugation to the nitrogen atoms of both TGs, while the π-electron conjugation at HOMO, HOMO−1, and HOMO−2 is spread out over the entire molecule. In total, seven MOs (from HOMO−4 to LUMO+1), shown in Fig. 8, are necessary for the quantum-chemical analysis.

It is commonly accepted that the electron transfer between the HOMO and LUMO ($1A_1 \rightarrow 1B_1$ transition) corresponds to the intense long-wavelength band in the 1PA spectrum. The next transition involving practically pure HOMO−1 and LUMO (see coefficients $T_{p,i\rightarrow j}$ in Table 1) and being of $1A_1 \rightarrow 2A_1$ symmetry should correspond to the lowest two-photon transition. However, based on the

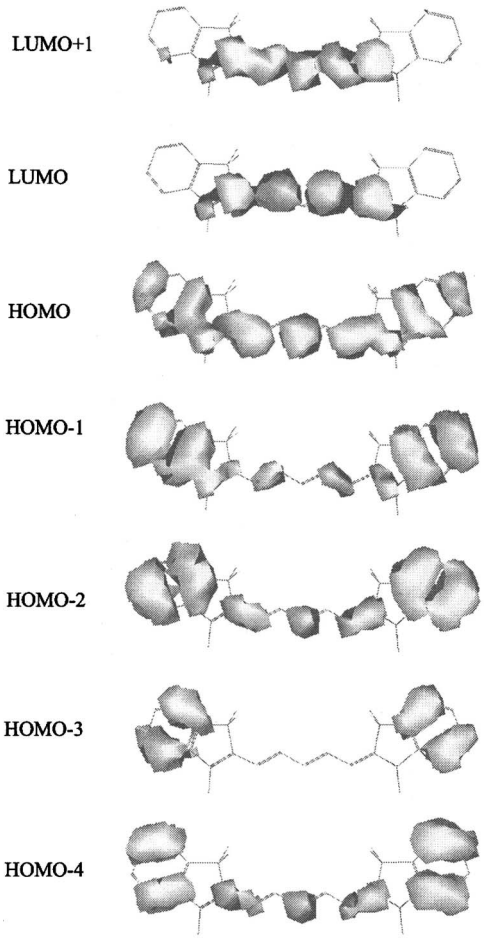

Fig. 8. Electron density distribution in the molecular orbitals for PD 2350.

results of the quantum-chemical calculations, we suggest that only the next $1A_1 \rightarrow 3A_1$ transition in Fig. 6 for PD2350, corresponding to the electron transfer between local HOMO−3 and delocalized LUMO, is the most active in 2PA for PD 2350 in agreement with the experimental spectral position of the second 2PA band seen in Fig. 1 at ≈390 nm. The main characteristic feature of the 2PA spectrum for the PDs is the relatively high δ_{2PA} of ≈700–1000 GM (as compared with dicarbocyanines with different TGs) owing to the strong coupling of these orbitals with the intermediate HOMO.

A slight spectral shift between the one-photon anisotropy dip and 2PA peak for PD 2350 can be explained by the overlap of the $1A_1 \rightarrow 3A_1$ ($S_0 \rightarrow S_4$, HOMO−3 →LUMO) one-photon forbidden transition with $1A_1 \rightarrow 2B_1$ ($S_0 \rightarrow S_3$, HOMO−2→LUMO) one-photon allowed transition shown in Table 1. For other types of TGs (for example, thiacarbocyanines[23]), both the one-photon anisotropy dip and the 2PA peak can coincide. The nature of the $1A_1 \rightarrow 4A_1$ ($S_0 \rightarrow S_6$ in Fig. 6 for PD2350) transition is connected with the transition between chain orbitals HOMO→LUMO+1 and cannot be reached experimentally owing to linear absorption.

To further increase the density of the occupied MOs and thus the number of electronic transitions, we choose TGs with more extended π-systems. This idea was realized in PD 2630 containing more complicated benzoindolium terminal groups. As compared with PD 2350, this dye is characterized by redshifted absorption bands. Note that experimentally the main 1PA peak is shifted by ≈0.1 eV, and the 2PA band is shifted more to the red by ≈0.18 eV. Because of this shift, the beginning of the next third 2PA band has been experimentally measured. Analyzing the evolution of the 2PA bands from the unsubstituted chain to PD 2350 and then to PD 2630, we assume that the spectral shift of the 2PA peak is due primarily to the terminal groups. More extended TGs may provide an additional shift, thus increasing the number of experimentally reachable 2PA bands.

B. Squaraines

An alternative way to increase the number of active two-photon transitions, $1A_1 \rightarrow mA_1$, can be provided by an increase of the density of unoccupied MOs. This has been achieved in the dyes of another type—squaraines. Inserting the strong acceptor C_4O_2 fragment in the center of the polymethine chain while keeping the same TGs can be chemically considered as a simultaneous cyclization of the chain by the C═O bridge and introduction of the anionic substituents O^- to the central position of the PD 2350 (or PD 2630). The latter makes the SD-molecule formally neutral or, more correctly, it can be considered as a bi-ionic molecule with separated positive and negative charges. As a result, shown in Fig. 5, the MOs of the neutral dye SD 2577 are shifted up in energy, and the distance between LUMO and LUMO+1 decreases as compared with the corresponding PD 2350. Therefore the energies of the electronic transitions involving LUMO+1 can be smaller than twice the energy of the transition $S_0 \rightarrow S_1$, i.e., the double-resonance energy. This change of the chemical structure of the chromophore center in SD 2577, as compared with PD 2350, also leads to a reassembling of its MOs as shown in Fig. 5.

In the case of SD 2577, five HOMOs and five LUMOs have to be considered to elucidate the nature of the allowed and forbidden transitions in the spectral area of interest (see Fig. 9). The nature of the allowed $S_0 \rightarrow S_1$ transition for SD 2577 remains the same as for the PDs and is connected with the electron transfer between HOMO and LUMO. Similar to PD 2350, two HOMO orbitals of both TGs for SD 2577 are also completely mixed with the orbitals of the chain producing HOMO−1 and HOMO−2. The HOMO−1 associated with each TG produce HOMO −3 and HOMO−4 in SD 2577 and remain mostly localized on the TGs with only a small participation of the chain.

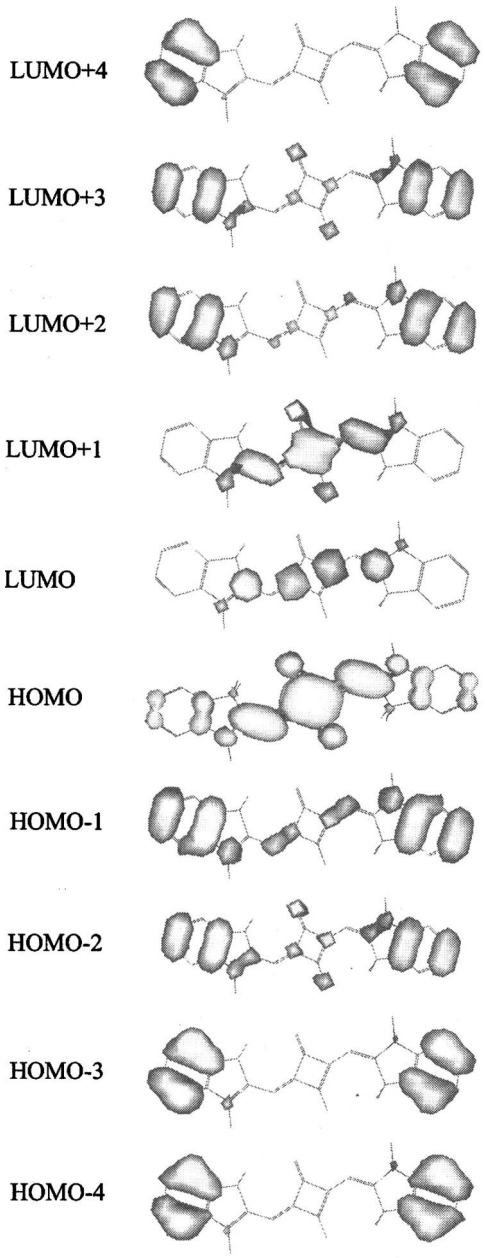

Fig. 9. Electron density distribution in the molecular orbitals for SD 2257.

For the neutral SD2577, the influence of the LUMOs associated with the TGs is very significant. Although the nature of LUMO and LUMO+1 is similar for PD2350 and SD2577, which preliminarily are associated with LUMOs from the chain, other unoccupied MOs are connected to LUMOs from the TGs, which mix with the MO located at the central C_4O_2.

Analysis of the quantum-chemical data shows that two electronic transitions are the most active for 2PA in agreement with the spectral positions of the measured bands. HOMO→LUMO+1 (presumably the $1A_g \rightarrow 4A_g$, $S_0 \rightarrow S_5$ transition in Fig. 6 for SD2577) was experimentally unreachable in PD2350 owing to linear absorption but is shifted to a lower energy region in the neutral SD2577 and thus becomes reachable. Also, the transition between the localized HOMO−3 and delocalized LUMO (presumably the $1A_g \rightarrow 5A_g$, $S_0 \rightarrow S_7$ transition in Fig. 6 for SD2577), which is analogous to the $1A_1 \rightarrow 3A_1$ transition in PD2350, is similarly shifted and can now be observed just below the linear absorption edge. These higher-lying $4A_g$ and $5A_g$ states are strongly coupled to the intermediate state as shown in Fig. 9.

The lower lying $3A_g$ state, connected with the charge distribution in the direction perpendicular to the long molecular axis, cannot be coupled to the intermediate state, and therefore the $1A_g \rightarrow 3A_g$ transition is not active in 2PA. As predicted, we did not observe this band experimentally. We do not observe the $1A_1 \rightarrow 2A_1$ transition for any of the dyes. This may be partially owing to the large detuning from the intermediate level S_1 leading to small 2PA.

C. Calculations

We reproduce the shape of the 2PA spectra for all the dyes by using the experimental and calculated molecular parameters shown in Table 2 and considering a simple extension of the three-state model proposed in Ref. 24. This model includes two final states ($f1$ and $f2$) and the same initial $S_0(0)$ and intermediate $S_1(1)$ states. This approximation is sufficient for organic molecules with a dominant $S_0 \rightarrow S_1$ transition and the limited number of electronic transitions between $S_0 \rightarrow S_1$ and its double-resonance position, especially if their excited states (such as in PDs and SDs) are practically pure with $T_{p,i\rightarrow j} \geq 0.9$ (see Table 1). Based on our calculations, all other terms except resonance terms [shown in Eq. (1)] in the sum-over-states expression for the imaginary part of third-order susceptibility can be ignored. Direct calculations show these terms to be at least two orders of magnitude smaller than the resonance terms' contributions.

Assuming that transition dipole moments μ_{01} and μ_{1f} are parallel to each other, the equation for δ_{2PA} at the laser frequency of v_p is

$$\delta_{2PA}(v_p) = \frac{64\pi^3}{5c^2h}\frac{{E_p}^2}{(E_{01}-E_p)^2+{\Gamma_{01}}^2}\left[\frac{|\mu_{01}|^2|\mu_{1f1}|^2\Gamma_{0f1}}{(E_{0f1}-2E_p)^2+{\Gamma_{0f1}}^2} + \frac{|\mu_{01}|^2|\mu_{1f2}|^2\Gamma_{0f2}}{(E_{0f2}-2E_p)^2+{\Gamma_{0f2}}^2}\right], \quad (1)$$

where c is the speed of light, h is Planck's constant, $E_p = hv_p$, $E_{01} = hv_{01}$, $E_{0f1} = hv_{0f1}$, $E_{0f2} = hv_{0f2}$ are the corresponding transition energies, and Γ is a damping constant.[21] As was noted in Ref. 10, if $1/2v_{0f2}$ is close to v_{01}, a very small detuning energy ($\Delta E = E_{01} - E_p$) occurs, leading to a dramatic enhancement of δ_{2PA}. All calculated spectra are presented in Figs. 1–4 and show a relatively good correlation with the measured 2PA.

Moreno and Kuzyk[25] used the general three-level model[26] combining a truncated Thomas–Kuhn sum rule to estimate the upper limit of 2PA cross sections of organic molecules. They used the normalized 2PA cross section to compare 2PA properties of different organic molecules that are calculated by normalizing the measured 2PA cross sections to the upper limit of 2PA. They also show that simply dividing by the square of the effective number of electrons per molecule yields a good metric for comparison. Based on their work,[27] we calculated the effective number of electrons for the four molecules we studied in this paper: $N_{eff}=15.2$ for PD2350, $N_{eff}=17.1$ for SD2577, $N_{eff}=19.9$ for PD2630, and $N_{eff}=21.7$ for SD2243. Figure 10 shows the comparison via normalized 2PA cross-sections. In this way we see that SDs exhibit experimentally observable larger normalized 2PA cross sections than their counterpart PDs. This is in large part owing to the fact that wavelengths closer to the linear absorption edge can be reached for SDs, thus increasing the resonance enhancement.

5. CONCLUSIONS

We have described a detailed experimental investigation and quantum-chemical analysis of the 2PA spectra of a se-

Table 2. Molecular Parameters for PD 2350, SD 2577, PD 2630, and SD 2243

Molecular Parameters	PD 2350	SD 2577	PD 2630	SD 2243	Method of Determination
Γ_{01}, eV	0.064	0.04	0.06	0.046	Experiment (HW1/eM)
Γ_{02}, eV	0.1	0.06	0.1	0.08	Estimation from experiment
Γ_{03}, eV	—	0.08	0.1	0.1	Estimation from experiment
E_{01}, eV	1.91	1.96	1.8	1.9	Experiment
E_{02}, eV	3.13	3.03	2.8	2.8	Experiment
E_{03}, eV	—	3.48	3.15	3.25	Experiment
μ_{01}, D	14.7	12.2	14.1	13.8	Experiment
μ_{12}, D	2.0	2.5	3.1	3.5	Best fit
μ_{13}, D	—	3.25	1.8	4.8	Best fit
$\Delta\mu$, D	2.6	1.45	2.8	2.0	Best fit

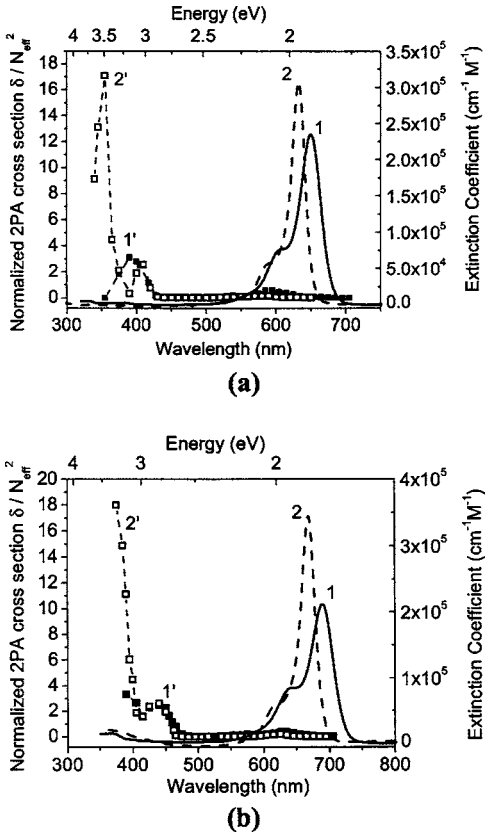

Fig. 10. 2PA comparison of PDs and SDs by normalized 2PA cross section Ref. 27. (a) PD2350 [(1), 1PA spectrum, (1′) normalized 2PA spectrum], SD2577 [(2) 1PA spectrum, (2′) normalized 2PA spectrum] (b) PD2630 [(1) 1PA spectrum, (1′) normalized 2PA spectrum], SD2243 [(2) 1PA spectrum, (2′) normalized 2PA spectrum].

ries of symmetrical cationic polymethines and neutral squaraines having similar structures. From the measurements we find that in the spectral region between the first absorption band and twice that energy there are two 2PA bands for PDs and three 2PA bands for SDs. Experimental and quantum-chemical analysis allows us to make the following conclusions:

1. For all the investigated molecules we observe a weakly allowed 2PA band within the vibronic shoulder of the first absorption band $S_0 \rightarrow S_1$. This band is forbidden by dipole selection rules for the symmetrical molecules; however, it displays 2PA with cross section $\delta_{2PA} \approx 40-160$ GM owing to molecular symmetry-breaking effects.

2. Introduction of the donor indolium terminal groups to the polymethine chain significantly increases the density of the occupied MOs and thus the number of electronic transitions between the first band, $S_0 \rightarrow S_1$, and its double-resonance position. Quantum-chemical analysis shows that electron transitions between the localized HOMO−3 and the delocalized LUMO (presumably the $1A_1 \rightarrow 3A_1$ transition) are the most active in 2PA for PDs, in agreement with the spectral positions of the measured bands. Relatively high $\delta_{2PA} \approx 700-1000$ GM can be observed owing to a strong coupling of these orbitals with the intermediate HOMO. The values of $\delta_{2PA} \approx 1000$ GM for the second 2PA peaks in PDs and SDs are comparable.

3. An alternative way to increase the number of active two-photon $1A_1 \rightarrow mA_1$ transitions can be provided by an increase of the density of unoccupied MOs. This has been achieved in the dyes of another type—squaraines. The distinguishing feature of SDs is the possibility to display an experimentally observable third and more intense 2PA band. This higher-lying third 2PA band in SDs displays much larger δ_{2PA} (more than 8600 GM) owing to a decrease in the detuning energy leading to a large enhancement of cross-section values, i.e., significant resonance enhancement of the 2PA cross section for both the intermediate and final states. This peak is observable just below the linear absorption edge.

4. The one-photon excitation fluorescence anisotropy spectrum can serve as a useful guide to indicate the approximate peak positions for 2PA bands.

ACKNOWLEDGMENTS

We gratefully acknowledge the support of the National Science Foundation ECS 0524533, the U.S. Army Research Laboratory (contract #W911NF0420012), and the U.S. Air Force Office of Scientific Research (contract #FA95500410200). O.V.P., M.V.B., A.D.K, and Yu.L.S. appreciate the partial support of the Civilian Research and Development Foundation (UK-C2-2574-KV-04).

J. Fu, the corresponding author, can be reached by e-mail at jfu@mail.ucf.edu.

REFERENCES

1. S. R. Marder, "Organic nonlinear optical materials: where we have been and where we are going," Chem. Commun. (Cambridge) **2006**, 131–134.
2. M. Albota, D. Beljonne, J. L. Bredas, J. E. Ehrlich, J.-Y. Fu, A. A. Heikal, S. Hess, T. Kogej, M. D. Levin, S. R. Marder, D. McCord-Maughon, J. W. Perry, H. Rockel, M. Rumi, G. Subramaniam, W. W. Webb, X.-L. Wu, and C. Xu, "Design of organic molecules with large two-photon absorption cross sections," Science **281**, 1653–1656 (1998).
3. T. Kogej, D. Beljonne, F. Meyers, J. W. Perry, S. R. Marder, and J. L. Bredas, "Mechanisms for enhancement of two-photon absorption in donor-acceptor conjugated chromophores," Chem. Phys. Lett. **298**, 1–3 (1998).
4. M. Rumi, J. E. Ehrlich, A. A. Heikal, J. W. Perry, S. Barlow, Z. Hu, D. McCord-Maughon, T. C. Parker, H. Rocker, S. Thayumanavan, S. R. Marder, D. Beljonne, and J. L. Bredas, "Structure-property relationships for two-photon absorbing chromophores: bis-donor diphenylpolyene and bis(styryl)benzene derivatives," J. Am. Chem. Soc. **122**, 9500–9510 (2000).
5. G. S. He, T.-C. Lin, J. Dai, P. N. Prasad, R. Kannan, A. G. Dombroskie, R. A. Vaia, and L.-S. Tan, "Degenerate two-photon-absorption spectral studies of highly two-photon active organic chromophores," J. Chem. Phys. **120**, 5275–5284 (2004).
6. C.-K. Wang, P. Macak, Y. Luo, and H. Agren, "Effects of π centers and symmetry on two-photon absorption cross sections of organic chromophores," J. Chem. Phys. **114**, 9813–9820 (2001).
7. E. Zojer, D. Beljonne, T. Kogej, H. Vogel, S. R. Marder, J. W. Perry, and J. L. Bredas, "Tuning the two-photon absorption response of quadrupolar organic molecules," J. Chem. Phys. **116**, 3646–3658 (2002).
8. E. Zojer, D. Beljonne, P. Pacher, and J. L. Bredas, "Two-photon absorption in quadrupolar π-conjugated molecules: influence of the nature of the conjugated bridge and the

donor-acceptor separation," Chem.-Eur. J. **10**, 2668–2680 (2004).
9. R. S. Lepkowicz, O. V. Przhonska, J. M. Hales, D. J. Hagan, E. W. Van Stryland, M. V. Bondar, Yu. L. Slominsky, and A. D. Kachkovski, "Excited-state absorption dynamics in polymethine dyes detected by polarization-resolved pump-probe measurements," Chem. Phys. **286**, 277–291 (2003).
10. J. M. Hales, D. J. Hagan, E. W. Van Stryland, K. J. Schafer, A. R. Morales, K. D. Belfield, P. Pacher, O. Kwon, E. Zojer, and J. L. Bredas, "Resonant enhancement of two-photon absorption in substituted fluorene molecules," J. Chem. Phys. **121**, 3152–3160 (2004).
11. M. Hamer, *The Cyanine Dyes and Related Compounds* (Interscience, 1964).
12. J. R. Lakowicz, *Principles of Fluorescence Spectroscopy* (Kluwer Academic/Plenum, 1999).
13. C. Xu and W. W. Webb, "Measurement of two-photon excitation cross sections of molecular fluorophores with data from 690 to 1050 nm," J. Opt. Soc. Am. B **13**, 481–491 (1996).
14. M. Fisher and J. Georges, "Fluorescence quantum yield of Rhodamine 6G in ethanol as a function of concentration using thermal lens spectrometry," Chem. Phys. Lett. **260**, 115–118 (1996).
15. M. Sheik-Bahae, A. A. Said, and E. W. Van Stryland, "High-sensitivity, single-beam n_2 measurements," Opt. Lett. **14**, 955–957 (1989).
16. M. Sheik-Bahae, A. A. Said, T.-H. Wei, D. R. Hagan, and E. W. Van Stryland, "Sensitive measurement of optical nonlinearities using a single beam," IEEE J. Quantum Electron. **26**, 760–769 (1990).
17. T. H. Wei, D. J. Hagan, M. J. Sence, E. W. Van Stryland, J. W. Perry, and D. R. Coulter, "Direct measurements of nonlinear absorption and refraction in solutions of phthalocyanines," Appl. Phys. B **54**, 46–51 (1992).
18. R. A. Negras, J. M. Hales, A. Kobyakov, D. J. Hagan, and E. W. Van Stryland, "Experiment and analysis of two-photon absorption spectroscopy using a white-light continuum probe," IEEE J. Quantum Electron. **38**, 1205–1216 (2002).
19. M. J. S. Dewar, *The Molecular Orbital Theory of Organic Chemistry* (McGraw-Hill, 1969).
20. J. S. Craw, J. R. Reimers, G. B. Bacskay, A. T. Wong, and N. S. Hush, "Solitons in finite- and infinite-length negative-defect trans-polyacetylene and the corresponding Brooker (polymethinecyanine) cations," Chem. Phys. **167**, 77–99 (1992).
21. D. Scherer, R. Dorfler, A. Feldner, T. Vogtmann, M. Schwoerer, U. Lawrentz, W. Grahn, and C. Lambert, "Two-photon states in squaraine monomers and oligomers," Chem. Phys. **279**, 179–207 (2002).
22. J. Fu, O. V. Przhonska, L. A. Padilha, D. J. Hagan, E. W. Van Stryland, K. D. Belfield, M. V. Bondar, Yu. L. Slominsky, and A. D. Kachkovski, "Two-photon anisotropy: analytical description and molecular modeling for symmetrical and asymmetrical organic dyes," Chem. Phys. **321**, 257–268 (2006).
23. J. Fu, O. V. Przhonska, L. A. Padilha, D. J. Hagan, E. W. Van Stryland, M. V. Bondar, Yu. L. Slominsky, and A. D. Kachkovski, unpublished results.
24. K. Kamada, K. Ohta, Y. Iwase, and K. Kondo, "Two-photon absorption properties of symmetric substituted diacetylene: drastic enhancement of the cross section near the one-photon absorption peak," Chem. Phys. Lett. **372**, 386–393 (2003).
25. J. P. Moreno and M. G. Kuzyk, "Fundamental limits of the dispersion of the two-photon absorption cross section," J. Chem. Phys. **123**, 194101–194113 (2005).
26. B. J. Orr and J. F. Ward, "Perturbation theory of the non-linear optical polarization of an isolated system," Mol. Phys. **20**, 513–526 (1971).
27. M. G. Kuzyk, "Fundamental limits on two-photon absorption cross sections," J. Chem. Phys. **119**, 8327–8334 (2003).